### Title

TCRα reporter mice reveal contribution of dual TCRα expression to T cell repertoire and function




### Journal

Proceedings of the National Academy of Sciences of the United States of America, 117(51)

### ISSN

0027-8424



### Authors

Yang, Letitia
Jama, Burhan
Wang, Huawei
et al.



### Publication Date

2020-12-22

### DOI

10.1073/pnas.2013188117

Peer reviewed

# TCRα reporter mice reveal contribution of dual TCRα expression to T cell repertoire and function

Letitia Yang[a], Burhan Jama[a], Huawei Wang[a], Lara Labarta-Bajo[b], Elina I. Zúñiga[b], and Gerald P. Morris[a,1]

[a]Department of Pathology, University of California San Diego, La Jolla, CA 92093; and [b]Division of Biological Sciences, University of California San Diego, La Jolla, CA 92093

Edited by Emil R. Unanue, Washington University in St. Louis School of Medicine, St. Louis, MO, and approved November 9, 2020 (received for review June 24, 2020)

**It is known that a subpopulation of T cells expresses two T cell receptor (TCR) clonotypes, though the extent and functional significance of this is not established. To definitively evaluate dual TCRα cells, we generated mice with green fluorescent protein and red fluorescent protein reporters linked to TCRα, revealing that ∼16% of T cells express dual TCRs, notably higher than prior estimates. Importantly, dual TCR expression has functional consequences, as dual TCR cells predominated response to lymphocytic choriomeningitis virus infection, comprising up to 60% of virus-specific CD4$^+$ and CD8$^+$ T cells during acute responses. Dual receptor expression selectively influenced immune memory, as postinfection memory CD4$^+$ populations contained significantly increased frequencies of dual TCR cells. These data reveal a previously unappreciated contribution of dual TCR cells to the immune repertoire and highlight their potential effects on immune responses.**

T cell receptor | TCR | T cell | LCMV

The T cell receptor (TCR) clonotype present on a T cell determines reactivity to specific peptide–major histocompatibility complex (pMHC) ligands, which in turn directs development, function, and homeostasis (1). Thus, T cell identity and function are intrinsically linked to TCR clonotype. Conventional T cells bear a single TCR clonotype formed as a heterodimer of TCRα and TCRβ proteins. However, a subset of T cells expresses two functional TCRαβ receptors (2–4). Coexpression of two TCRs results from incomplete allelic exclusion of TCRα and TCRβ gene loci during thymopoiesis (4–7). A prevailing view of dual TCR expression as a by-product of TCR gene rearrangement posits that it affects only a small (1 to 10%) subset of T cells and does not have significant functional consequence. However, a growing body of evidence indicates that dual TCRα-expressing T cells contain a unique repertoire of TCRα clonotypes (8) and that these cells may have distinct potential to respond to ligands such as auto- or alloantigens (8–18). Despite evidence of the involvement of dual TCRα cells in pathogenic responses including autoimmunity and graft-versus-host disease, they remain understudied due to limitations in definitively identifying and isolating these cells.

Transgenic TCR systems have demonstrated the potential for dual TCR coexpression to enable emergence of pathologic dual receptor cells bearing clonotypes that would otherwise be eliminated during thymic selection (9, 11, 14, 15, 17). However, the effect of dual TCR coexpression on naturally developing T cell repertoires has been more difficult to evaluate. Genetic elimination of dual TCRα expression, commonly by knockout of one chromosomal copy of *TRAC*, has exhibited heterogenous effects on T cell development and function (8, 10, 16, 19). Studies based on genetic elimination of dual TCRα cells may not accurately reflect the role of dual receptor cells in normal physiology, as the breadth of the TCR repertoire could compensate for loss of specific subsets. Evaluation of dual TCRα cells in intact T cell repertoires has relied on pairwise labeling with monoclonal antibodies (mAbs) against TCRVα (2, 4). This approach is critically limited by a paucity of reagents (covering only ∼13% of mouse and human TCRVα), requiring extrapolation and potentially biased estimation of dual TCRα cells. Single-cell RNA sequencing can provide unbiased evaluation of cells with two TCR gene rearrangements, though analysis pipelines often filter multiple TCR sequences from individual cells (20–22), leading to underestimation of dual TCR cell frequencies. Furthermore, presence of in-frame TCR gene rearrangements may not necessarily translate into functional protein (23). Finally, single-cell sequencing is a terminal event for the cells studied and precludes further functional testing, hindering mechanistic investigation.

To overcome these limitations, we generated transgenic B6.TCRA-GFP/RFP (green fluorescent protein/red fluorescent protein) mice with TCRα protein generated from one chromosomal copy of *TRAC* labeled with GFP and TCRα protein generated from the other chromosomal copy labeled with RFP. Using this system, single and dual TCRα cells are unequivocally identifiable. This system defines dual TCRα cells as a much larger component of the naive T cell repertoire than previously appreciated. Importantly, this system enables the discovery that dual TCRα cells have a selective contribution to protective immune response and subsequent memory formation during viral infection.

## Results

**Generation of Fluorophore-Tagged TCRα Reporter Mice.** Most (>90%) dual TCR cells result from production of two functional TCRα proteins (2, 3), each paring with the cell's single TCRβ. To overcome the limitations of existing approaches for identification of single- and dual-TCR cells, we used CRISPR-Cas9–mediated gene editing (24) to insert genes encoding enhanced GFP (GFP) and tdTomato (RFP) at the 3′ end of exon 3 of *TRAC* [exon 4 is not translated (25)] to generate two transgenic mouse lines

### Significance

**This study utilizes novel transgenic reporter mice to definitively evaluate T cells coexpressing two T cell antigen receptors. These experiments demonstrate that T lymphocytes naturally coexpressing two different antigen receptors are significantly more abundant than previous estimates and that these cells have a previously unappreciated role in physiologic immune responses.**

Author contributions: L.Y., H.W., L.L.-B., E.I.Z., and G.P.M. designed research; L.Y., B.J., H.W., and G.P.M. performed research; L.L.-B. and E.I.Z. contributed new reagents/analytic tools; L.Y., H.W., L.L.-B., E.I.Z., and G.P.M. analyzed data; and L.Y., L.L.-B., E.I.Z., and G.P.M. wrote the paper.

The authors declare no competing interest.

This article is a PNAS Direct Submission.



[1]To whom correspondence may be addressed. Email: gpmorris@ucsd.edu.

This article contains supporting information online at https://www.pnas.org/lookup/suppl/doi:10.1073/pnas.2013188117/-/DCSupplemental.

First published December 7, 2020.

(*SI Appendix*, Fig. S1*A*). Reporter genes were attached to the C-terminal end of TCRCα by an 18-amino-acid flexible linker protein to colocalize reporters to the TCRα while avoiding interference with TCR trafficking or function (26). Double-stranded DNA plasmid containing reporter gene constructs flanked by 1-kb homology arms of genomic *TRAC* sequence, CRISPR RNA, guide RNA, and Cas9 protein were injected by micropipette into ∼200 C57BL/6 (B6) embryos. Flow cytometry of peripheral blood leukocytes identified 1/11 pups expressed TCRα-GFP and 1/26 pups expressed TCRα-RFP. Founder mice with individual reporters were bred to generate B6.TCRA-GFP and B6.TCRA-RFP lines homozygous for TCRα reporters.

The insertion site of the GFP and RFP reporter genes was confirmed by sequencing of the flanking DNA regions. Expression of GFP and RFP in transgenic mice is specific for $CD4^+$ and $CD8^+$ T cells (*SI Appendix*, Fig. S1*B*). Confocal microscopy confirmed that GFP and RFP reporters localize to the T cell membrane (*SI Appendix*, Fig. S1*C*). GFP and RFP reporters are first detectable at low levels in double-positive $CD4^+CD8^+$ (DP) thymocytes and increase in expression throughout maturation to single-positive $CD4^+CD8^-$ (CD4SP) and $CD4^-CD8^+$ (CD8SP) thymocytes (*SI Appendix*, Fig. S1 *D–F*), consistent with increasing TCRα expression during thymopoiesis. B6.TCRA-GFP and B6.TCRA-RFP mice had normal thymic development, with equivalent generation of CD4SP and CD8SP thymocytes at frequencies similar to wild-type B6 mice (*SI Appendix*, Fig. S1*G*). Reporter mice had normal frequencies of $CD4^+$ and $CD8^+$ T cells in the spleen (*SI Appendix*, Fig. S1*H*). $CD4^+$ and $CD8^+$ T cells from reporter mice proliferated equivalently to T cells from wild-type B6 mice following in vitro stimulation with plate-bound anti-CD3 and anti-CD28 (*SI Appendix*, Fig. S1 *I* and *J*), indicating that GFP and RFP do not interfere with TCR function.

**B6.TCRA-GFP/RFP Mice Reveal High Frequency of Dual TCR Expression.** B6.TCRA-GFP and B6.TCRA-RFP mice enable evaluation of the entire repertoire of TCRα expression by flow cytometry, removing the limitation of anti-TCRVα mAb labeling. Interbreeding TCRα reporter transgenic lines to produce mice with one *TRAC* chromosomal copy containing the GFP reporter and the other containing the RFP reporter (B6.TCRA-GFP/RFP) provided the ability to distinguish T cells expressing a single GFP or RFP TCRα from those coexpressing two TCRα chains. Flow cytometry of splenocytes from B6.TCRA-GFP/RFP mice clearly identified populations of $CD4^+$ and $CD8^+$ T cells coexpressing GFP- and RFP-labeled TCRα (Fig. 1*A*). The frequency of $GFP^+RFP^+$ dual receptor cells was significantly higher than established consensus estimates of 1 to 10% (2–4), with 16.7 ± 1.3% of $CD4^+$ and 16.9 ± 0.9% (mean ± SD) of $CD8^+$ T cells coexpressing dual TCRα (Fig. 1*B*). Confocal microscopy demonstrated colocalization of TCRα-GFP and TCRα-RFP at the cell membrane in $GFP^+RFP^+$ cells (Fig. 1*C*). This suggests that the high frequency of dual GFP and RFP expression measured by flow cytometry is not a result of nonproductive TCRα protein not expressed on the cell surface but represents true coexpression. The frequency of dual-$GFP^+RFP^+$ T cells identified by confocal microscopy was 16.0 ± 1.0% (Fig. 1*D*), similar to that observed by flow cytometry. However, it is possible that cells appearing as single-TCRα cells have low levels of a second TCRα protein below the threshold for detection by these methods, suggesting that the frequencies of dual TCRα cells detected here represent minimums with a possibility for cells expressing very low levels of second TCRα proteins.

Cell-surface expression of TCR proteins is a dynamic process, which can be both negatively and positively regulated (27). Studies in Jurkat cells have demonstrated that cell-surface levels of coexpressed TCRs can be differentially regulated during T cell stimulation (28), and nonengaged TCRαβ proteins can be actively recruited to the immune synapse at the cell surface (29). To examine the potential for single $GFP^+$ or $RFP^+$ cells to harbor second TCRα proteins that could be up-regulated to the cell surface, we isolated $GFP^+RFP^-$ and $GFP^-RFP^+$ T cells from B6.TCRA-GFP/RFP mice by FACS (fluorescence-activated cell sorting) and examined TCRα coexpression following 5-d stimulation with anti-CD3/anti-CD28 mAbs (*SI Appendix*, Fig. S2 *A* and *B*). In vitro stimulation resulted in 3.3 ± 1.0% of $GFP^+RFP^-$ and 1.2 ± 0.5% of $GFP^-RFP^+$ cells expressing a second TCRα detectable by flow cytometry. We do not attribute changes in reporter expression to induced transcription/translation of nonfunctional *TRAV-J* rearrangements, as the fluorophore reporters are linked to TCRCα as single-chain proteins and nonproductive rearrangements would likely result in the protein's being out of frame for translation. We also do not attribute dual TCRα expression to trogocytosis (30), as in vitro stimulation of cocultured T cells from B6.TCRA-GFP and B6.TCRA-RFP mice did not produce dual $GFP^+RFP^+$ cells (*SI Appendix*, Fig. S2 *C* and *D*). These data support that our dual-transgenic system robustly identifies single- and dual-TCRα T cells.

**Expression of Dual TCRα Is Associated with Positive Selection of DP Thymocytes.** Coexpression of dual TCRα results from a lack of TCRα allelic exclusion in DP thymocytes. It has been presumed that ∼33% of thymocytes have two in-frame *TRAV-J* rearrangements capable of producing functional TCRα protein, though frequencies of mature thymocytes coexpressing two TCRα proteins measurable by mAb labeling is significantly lower at 5 to 7% (23). Similar to results from identification of dual TCRα peripheral T cells (Fig. 1), flow cytometry analysis of thymocytes from B6.TCRA-GFP/RFP mice demonstrates significantly higher frequencies of dual TCRα CD4SP (18.0 ± 1.4%) and CD8SP (19.5 ± 2.0%) (Fig. 2 *A* and *B*) than previously estimated.

The ability to recombine *TRAV-J* on both chromosomal loci and express dual TCRα has been associated with facilitating positive selection and promoting production of mature CD4SP and CD8SP (8, 19). However, these results are from $TRAC^{+/-}$ systems, which may not directly reflect the effect of dual TCRα expression; decreased positive selection and thymocyte maturation associated with loss of dual-chromosome *TRAV-J* recombination may reflect an inability to generate a single productive TCRα rather than an increased ability of dual TCRα cells to successfully undergo positive selection. To investigate this, we measured the frequency of dual TCRα expression in $TCR^{low}CD69^+$, $TCR^{high}CD69^+$, and $TCR^{high}CD69^{low}$ stages of DP thymocytes selection (GFP and RFP reporter expression in $TCR^{low}CD69^-$ DP thymocytes was beneath the threshold for reliable detection by flow cytometry; *SI Appendix*, Fig. S1 *D–F*) (Fig. 2 *C* and *D* and *SI Appendix*, Fig. S3*A*). Compared to preselection $TCR^{low}CD69^+$ cells (14.0 ± 5.6%), dual TCRα frequency was significantly increased among $TCR^{high}CD69^+$ (22.6 ± 6.1%, $P < 0.05$) and $TCR^{high}CD69^{low}$ DP thymocytes successfully undergoing positive selection (18.3 ± 8.5%, $P < 0.05$). These data are consistent with previous findings and suggest that dual TCRα protein expression, rather than just the ability to recombine two sets of *TRAV-J* gene segments, promotes positive selection.

The positive effect of dual TCRα coexpression on positive selection contrasts with a paradoxical observation that dual TCRα expression impairs agonist selection of regulatory $FoxP3^+CD4^+$ T cells (Treg) (19). Agonist selection of thymocytes, essential for thymic generation of Tregs, invariant natural killer T (NKT) cells, and $CD8\alpha\alpha^+$ intraepithelial T cells, results from high-affinity interactions with self-pMHC ligands (31). Thymic Tregs in B6.TCRA-GFP/RFP mice demonstrated frequencies of dual TCRα expression similar to CD4SP thymocytes (Fig. 2 *E* and *F*). Thymic NKT cells had similar frequencies of

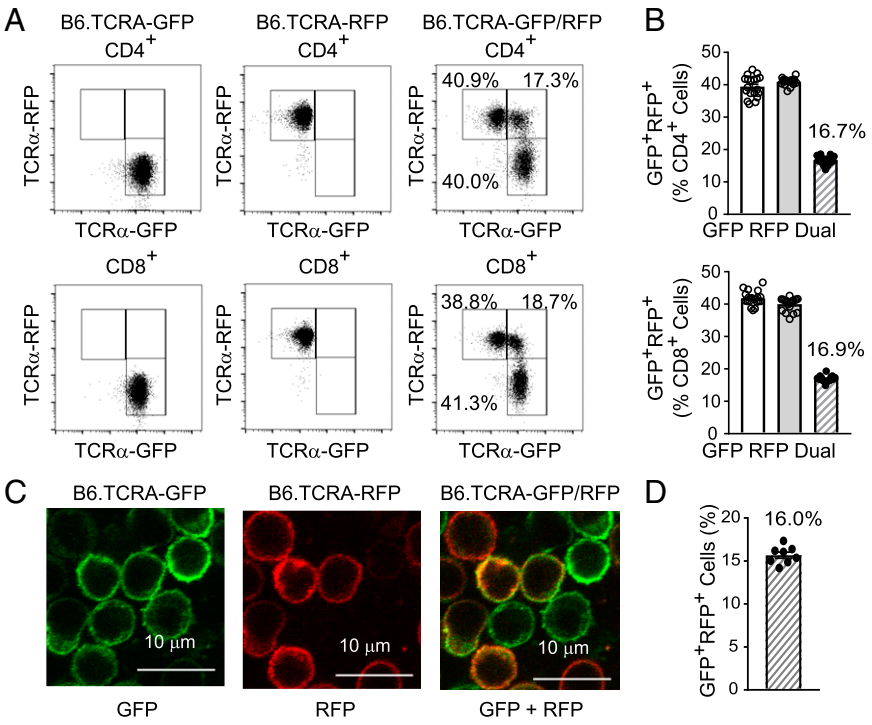


**Fig. 1.** B6.TCRA-GFP/RFP mice identify high frequency of dual TCRα cells. (*A*) Identification of GFP$^+$, RFP$^+$, and dual GFP$^+$RFP$^+$ cells from adult B6.TCRA-GFP, B6.TCRA-RFP, and B6.TCRA-GFP/RFP mice. Representative samples shown. (*B*) Quantification of TCRA-GFP$^+$, TCRA-RFP$^+$, and dual TCRA-GFP$^+$RFP$^+$ CD4$^+$ and CD8$^+$ T cells. Dots represent 19 individual mice from six independent experiments, mean ± SEM. (*C*) Confocal microscopy of T cells from B6.TCRA-GFP/RFP mice. Images shown for GFP and RFP channels and merged channels for a representative single field at 600× magnification. (*D*) Quantification of TCRA-GFP$^+$, TCRA-RFP$^+$, and TCRA-GFP$^+$RFP$^+$ T cell-enriched splenocytes identified by manual counting of 10 confocal microscopy image fields containing 300 to 1,000 cells per image field per sample. Dots represent eight individual mice from three independent experiments, mean ± SEM.

dual TCRα expression (*SI Appendix*, Fig. S3 *B* and *C*). Consistent with the lack of observable effect of dual TCRα expression on agonist selection, we did not observe increased expression of CD5, a surrogate marker for TCR signal strength in response to positively selecting self-pMHC (32–34), on dual TCRα CD4SP or CD8SP (*SI Appendix*, Fig. S3 *D* and *E*). These data suggest that while dual TCRα expression promotes recognition of self-pMHC during positive selection it may not result in a generally increased affinity/avidity for selecting pMHC ligands.

**Dual TCR T Cells Have Unchanged Total TCR Expression and Function but Increased CD5.** Previous descriptions of TCR allelic inclusion have indicated that coexpression of two TCR clonotypes does not increase total antigen receptor expression at the cell surface (2, 35). This likely results from TCR complex stoichiometry regulating cell-surface expression via limited availability of CD3 proteins (36). Measurement of CD3 by flow cytometry as an assessment of total TCR expression confirmed that GFP$^+$RFP$^+$ dual TCRα cells expressed similar amounts of CD3 as compared to single TCR cells (Fig. 3 *A* and *B*). Similarly, coexpression of two TCR clonotypes had no effect on T cell response to non-specific TCR stimulation, as graded doses of anti-CD3/anti-CD28 mAbs or staphylococcal enterotoxin B (SEB) resulted in equivalent in vitro proliferation of single and dual TCRα cells (*SI Appendix*, Fig. S4). These data confirm previous observations that coexpression of two TCR clonotypes does not confer a general advantage for TCR stimulation (14, 18, 35).

TCR is required not only for recognition of foreign antigens but also for recognition of self-pMHC ligands for homeostatic maintenance of T cells (1). The affinity of this interaction can be estimated as proportionate to the cell-surface expression of CD5 (34). We have previously demonstrated that dual TCRα cells identified by anti-TCRVα mAb colabeling express higher levels of CD5 than single TCRα cells. This correlates with increased dual TCRα T cell potential for acute lymphopenia-induced proliferation (35), a function dependent on TCR interaction with self-pMHC ligands (37, 38). Similar to our previous investigations, dual TCRα cells from B6.TCRA-GFP/RFP mice demonstrated increased expression of CD5 on the cell surface as compared to single TCRα CD4$^+$ and CD8$^+$ cells (Fig. 3 *C* and *D*). This effect was more pronounced in CD4$^+$ dual TCRα cells, which had an average 31.6% higher expression of CD5 than single TCRα cells from the same mouse. Comparatively, CD8$^+$ dual TCRα cells demonstrated an average 12.4% increase in CD5 expression. This contrasts to the absence of any difference in CD5 expression by dual TCRα CD4SP or CD8SP (*SI Appendix*, Fig. S3 *D* and *E*). However, CD5 expression and its effects on TCR signaling can be changed in response to self-pMHC–induced tonic signaling in the periphery (39), providing a plausible explanation for this apparent discrepancy.

Increased expression of CD5 by dual TCRα T cells in the periphery suggests that they may have an increased reactivity with self-antigens. However, dual TCRα coexpression was not observed at increased frequencies among T cell subsets associated with reactivity against self-ligands including splenic Tregs (*SI Appendix*, Fig. S5 *A* and *B*), NKT cells (*SI Appendix*, Fig. S5 *C* and *D*), intestinal CD4$^+$ and CD8$^+$ T cells (*SI Appendix*, Fig. S5 *G* and *H*), intestinal Tregs (*SI Appendix*, Fig. S5 *I* and *J*), and CD8αα$^+$ T cells (*SI Appendix*, Fig. S5 *K* and *L*). The frequency of splenic T cells from immunologically naive mice expressing high levels of CD44, a marker of prior activation in response to antigen, was also similar between single and dual TCR CD4$^+$ and CD8$^+$ T cells from immunologically naive B6.TCRA-GFP/RFP mice (Fig. 3 *E* and *F*). Similarly, dual TCRα cells were not

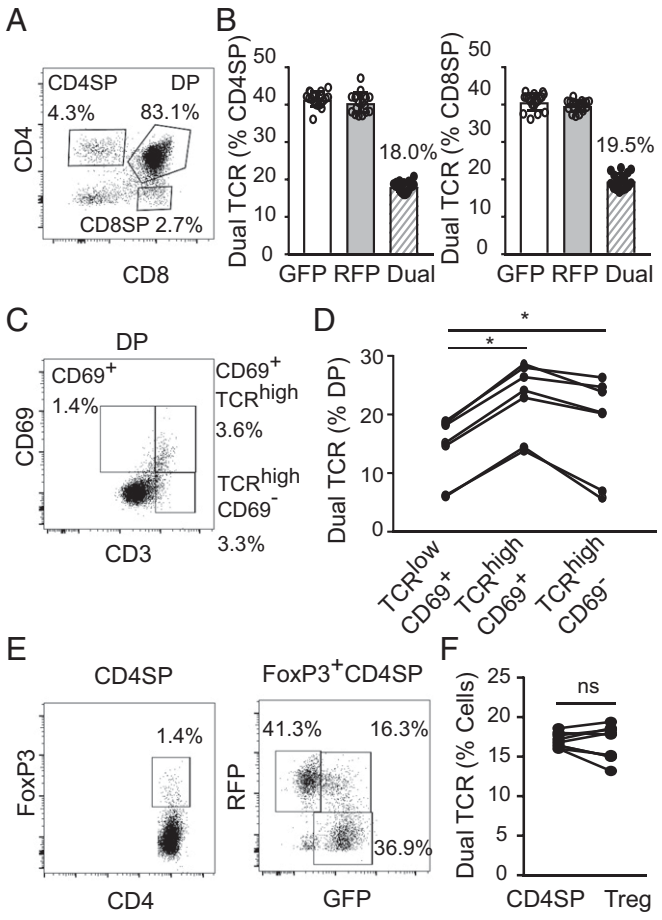


**Fig. 2.** Dual TCRα expression arises during positive selection of thymocytes. (*A*) $CD4^+CD8^+$ DP, $CD4^+CD8^-$ single-positive (CD4SP), and $CD4^-CD8^+$ single-positive (CD8SP) thymocytes were identified from B6.TCRA-GFP/RFP mice by flow cytometry. Representative sample shown. (*B*) Quantification of dual TCRα $GFP^+RFP^+$ CD4SP and CD8SP. Dots represent 16 individual mice from six independent experiments, mean ± SEM. (*C*) $TCR^{low}CD69^+$, $TCR^{high}CD69^+$, and $TCR^{high}CD69^{low}$ maturation stages of DP thymocytes were identified by flow cytometry. Representative sample shown. (*D*) Quantification of dual TCRα $GFP^+RFP^+$ DP thymocytes related to developmental stage. Linked dots represent seven individual mice from three independent experiments. Data compared by Wilcoxon matched-pairs rank-sign test. (*E*) Thymic $CD4^+FoxP3^+$ Tregs were identified among CD4SP by flow cytometry. Representative sample shown. (*F*) Quantification of dual TCRα $GFP^+RFP^+$ CD4SP Tregs. Dots represent nine individual mice from three independent experiments, mean ± SEM. Data compared by Wilcoxon matched-pairs rank-sign test. $*P < 0.05$; ns = not statistically significant.

observed at increased frequencies among $CD44^{high}CD62L^-$ effector memory (EM) or $CD44^{low}CD62L^+$ central memory (CM) cells in immunologically naive mice (*SI Appendix*, Fig. S5 *E* and *F*). However, dual TCRα T cells in the spleen were more frequently positive for the early activation marker CD69 ($CD4^+$ 10.0 ± 2.7% dual TCRα vs. 5.8 ± 1.6% single TCRα, $P < 0.005$; $CD8^+$ 2.2 ± 1.1% dual TCRα vs. 1.3 ± 0.4% single TCRα, $P < 0.005$) (Fig. 3 *G* and *H*). Concurrently, a higher proportion of dual TCRα $CD4^+$ cells had an anergy-associated $CD73^{high}FR4^{high}$ phenotype (40) (6.6 ± 2.3% dual TCRα vs. 3.2 ± 1.3% single TCRα, $P < 0.005$) (Fig. 3 *I* and *J*). Together these data support a model where dual TCRα expression may promote increased reactivity against self-pMHC antigens, but the biologic effect is limited at an immunologic steady state via up-regulation of the negative regulator of TCR signaling CD5 and induction of anergy.

**Dual TCR Expression Promotes Protective Immune Response to Lymphocytic Choriomeningitis Virus Infection.** Identification of dual TCRα populations significantly larger than previous estimates suggests that there may be unappreciated effects of dual receptor expression on immune responses. To examine the role of dual TCRα cells in a protective immune response, B6.TCRA-GFP/RFP mice were infected with murine lymphocytic choriomeningitis virus (LCMV) Armstrong strain. Infected mice were killed 8 d after infection to evaluate the acute immune response (41). Dual TCRα cells were increased in the spleen and lymph nodes for total dual TCRα $CD4^+$ cells (23.8 ± 3.9%, $P < 0.001$) and $CD8^+$ cells (23.4 ± 5.3%, $P < 0.005$) compared to immunologically naive mice (Fig. 4*A*). This indicates a potential advantage for dual TCRα expression during an immune response, though antigen specificity in the broad population is undefined.

LCMV-specific T cells were identified from spleen and lymph node cells by flow cytometry for binding I-$A^b$:$GP_{66–77}$ and H2-$D^b$:$GP_{33–41}$ tetramers (Fig. 4 *B* and *C*). While labeling with these tetramers does not exhaustively identify all LCMV-specific T cells, it enables examination of defined LCMV-specific T cells. Focusing on the LCMV-specific response revealed more dramatic expansion of virus-specific dual TCR cells during infection. LCMV $tetramer^+$ $CD4^+$ and $CD8^+$ cells contained significantly higher frequencies of dual TCRα cells ($CD4^+$ 48.1 ± 11.1%, $P < 0.005$; $CD8^+$ 36.5 ± 8.7%, $P < 0.005$) than tetramer-negative populations within individual mice (Fig. 4 *D* and *E*). Dual TCRα cell populations in tetramer-negative cells were increased as compared to uninfected mice ($CD4^+$ 22.4 ± 3.0%, $P < 0.05$; $CD8^+$ 25.0 ± 4.8%, $P < 0.05$), similar to the observed effect in total T cells (Fig. 4*A*). This likely reflects a broad response against multiple LCMV antigens. The dramatic specific expansion of LCMV-specific dual TCRα cells in $tetramer^+$ populations demonstrates a selective benefit of dual TCRα expression to the protective immune response.

Within LCMV tetramer-specific T cell populations, dual TCRα expression directed differing phenotypes for $CD4^+$ and $CD8^+$ T cells. LCMV-specific $CD4^+$ dual TCRα cells had higher frequencies of $CD11a^+CD49d^+$ cells, associated with an activated T cell response during acute LCMV infection (42), compared to single TCRα cells from the same mouse (Fig. 4 *F* and *G*). In LCMV-specific $CD8^+$ cells, dual TCRα expression also affected effector cell differentiation, though in an opposite manner than for $CD4^+$ cells (Fig. 4 *H* and *I*), as dual TCRα expression was associated with lower frequencies of $KLRG\text{-}1^{high}Ly6c^+$ terminal effector $CD8^+$ cells (43). These data suggest that while dual TCRα expression may promote responses in both $CD4^+$ and $CD8^+$ T cells, dual TCRα expression may differentially affect the nature of those responses.

Binding of pMHC tetramers is considered indicative of reactivity against a specific antigen. However, tetramer can have nonspecific binding with T cells that do not have measurable functional response against the antigen or, conversely, can miss antigen-specific T cells with low affinity for antigen (44, 45). To address this, functional responses against LCMV were assessed by measurement of cytokine production after ex vivo antigen-specific stimulation of splenocytes from infected mice. Similar to the tetramer data, $CD4^+$ dual TCRα cells from infected mice demonstrated a preferential functional response. Stimulation of splenocytes with LCMV $GP_{66–77}$ peptide resulted in higher frequencies of dual TCRα cells producing interferon gamma (IFNγ) and tumor necrosis factor alpha (TNFα) compared to single TCRα cells in the same culture (Fig. 5 *A* and *B*). Responding single and dual TCRα cells produced equivalent levels of cytokine on a per-cell basis (*SI Appendix*, Fig. S6*A*). Dual TCRα expression had similar effects on cytokine production by $CD8^+$ cells in response to LCMV $GP_{33–41}$ stimulation. Dual TCRα cells had higher frequencies of cells producing IFNγ and TNFα but not granzyme B in response to antigenic stimulation (Fig. 5 *C*

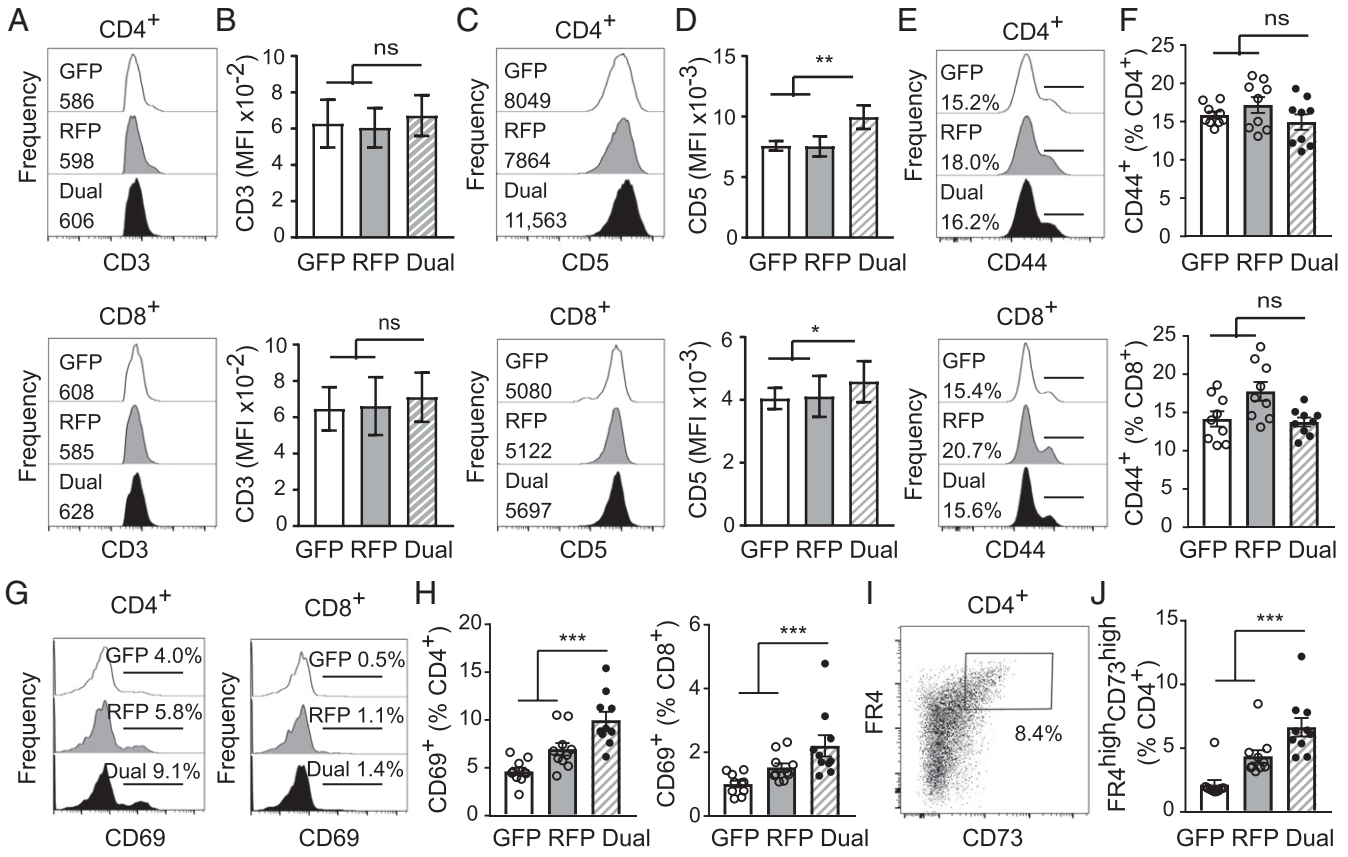


**Fig. 3.** Dual TCR cells have equivalent total TCR but increased CD5. CD4$^+$ and CD8$^+$ splenic T cells from TCRA-GFP$^+$, TCRA-RFP$^+$, and TCRA-GFP$^+$RFP$^+$ mice were examined by flow cytometry. (*A*) Comparison of CD3 expression by GFP$^+$, RFP$^+$, and GFP$^+$RFP$^+$ cells with MFI from single representative sample shown. (*B*) Aggregate data for CD3 expression of nine mice from three independent experiments, mean ± SD. Data compared using paired Student's *t* test. (*C*) Comparison of CD5 expression on GFP$^+$, RFP$^+$, and GFP$^+$RFP$^+$ cells with MFI from single representative sample shown. (*D*) Aggregate data for CD5 expression of nine mice from three independent experiments, mean ± SD. Data compared using paired Student's *t* test. (*E*) Comparison of CD44 expression by GFP$^+$, RFP$^+$, and GFP$^+$RFP$^+$ cells with percentages of CD44$^+$ cells from single representative sample shown. (*F*) Aggregate frequencies of CD44$^+$ cells. Dots represent nine individual mice from three independent experiments, mean ± SD. Data compared using Wilcoxon matched-pairs rank-sign test. (*G*) Comparison of CD69 expression by GFP$^+$, RFP$^+$, and GFP$^+$RFP$^+$ cells with percentages of CD69$^+$ cells from single representative sample shown. (*H*) Aggregate frequencies of CD69$^+$ cells. Dots represent nine individual mice from three independent experiments, mean ± SEM. Data compared using Wilcoxon matched-pairs rank-sign test. (*I*) Identification of CD73$^{high}$FR4$^{high}$ CD4$^+$ T cells as a marker for anergic phenotype. Representative sample shown, with single TCRα GFP$^+$ or RFP$^+$ cells in gray and dual TCRα GFP$^+$RFP$^+$ cells in black. (*J*) Dots represent nine individual mice from three independent experiments, mean ± SEM. Data compared using Wilcoxon matched-pairs rank-sign test. *$P < 0.05$, **$P < 0.01$, ***$P < 0.001$; ns = not statistically significant.

and *D*). Responding single and dual TCRα CD8$^+$ cells produced equivalent amounts of cytokines (*SI Appendix*, Fig. S6*B*). These data are consistent with the LCMV tetramer data and support that dual TCRα expression favors functional participation in the protective antiviral immune response. The data also indicate that dual TCRα cells do not have an increased functional capacity but rather an increased ability to respond to antigen.

**Dual TCR Expression Differentially Affects Persistence and Memory of CD4$^+$ and CD8$^+$ T Cell Immune Responses.** In the acute phase of the immune response against LCMV, dual TCRα expression promoted participation in the immune response for both CD4$^+$ and CD8$^+$ T cells. We evaluated whether dual TCRα expression persistently affected the antiviral immune response by examining dual TCRα T cells 28 d after infection with LCMV Armstrong (Fig. 6*A*). Dual TCRα CD4$^+$ T cells (20.0 ± 1.9%, $P < 0.001$) remained increased compared to immunologically naive mice. Conversely, dual TCRα CD8$^+$ T cells (16.8 ± 2.9%) returned to baseline frequencies. This pattern was consistent when examining LCMV-specific T cells identified by flow cytometry for binding I-A$^b$:GP$_{66–77}$ and H2-D$^b$:GP$_{33–41}$ tetramers (Fig. 6 *B* and *C*). At 28 d after infection, LCMV-specific dual TCRα cells remained significantly increased among LCMV tetramer$^+$ CD4$^+$ T cells (33.8 ± 11.7%, $P < 0.005$) as compared to tetramer-negative cells, while CD8$^+$ cells did not demonstrate the same persistence of LCMV tetramer$^+$ dual TCRα cells (13.5 ± 5.3%).

LCMV-specific dual TCRα cells among both CD4$^+$ and CD8$^+$ T cells predominantly (78.4 ± 16.7% and 89.3 ± 7.6%) had an EM phenotype 28 d after infection (Fig. 6*D*). Examining EM and CM cells after resolution of LCMV infection revealed that dual TCRα cells were markedly increased in both total and I-A$^b$:GP$_{66–77}$–specific EM (total 26.7 ± 1.6%, Tet$^+$ 32.6 ± 12.6%) and CM (total 25.7 ± 11.0%, Tet$^+$ 41.6 ± 24.6%) CD4$^+$ populations (Fig. 6*E*). A similar effect was not seen for CD8$^+$ EM and CM populations, where dual TCRα cells were found at frequencies similar to preinfection (total EM 18.0 ± 3.8%, Tet$^+$ EM 12.5 ± 3.7%, total CM 15.1 ± 3.4%, Tet$^+$ CM 18.1 ± 9.9%). While dual TCRα expression did not seem to provide a benefit to the persistence of LCMV-specific CD8$^+$ cells or their differentiation into memory cells, the difference between dual TCRα cell frequency among total CD4$^+$ T cells, which returned to preinfection frequencies after the resolution of infection, and the increased frequency of dual TCRα cells among total CD4$^+$ EM and CM cells indicates that dual TCRα expression affects the

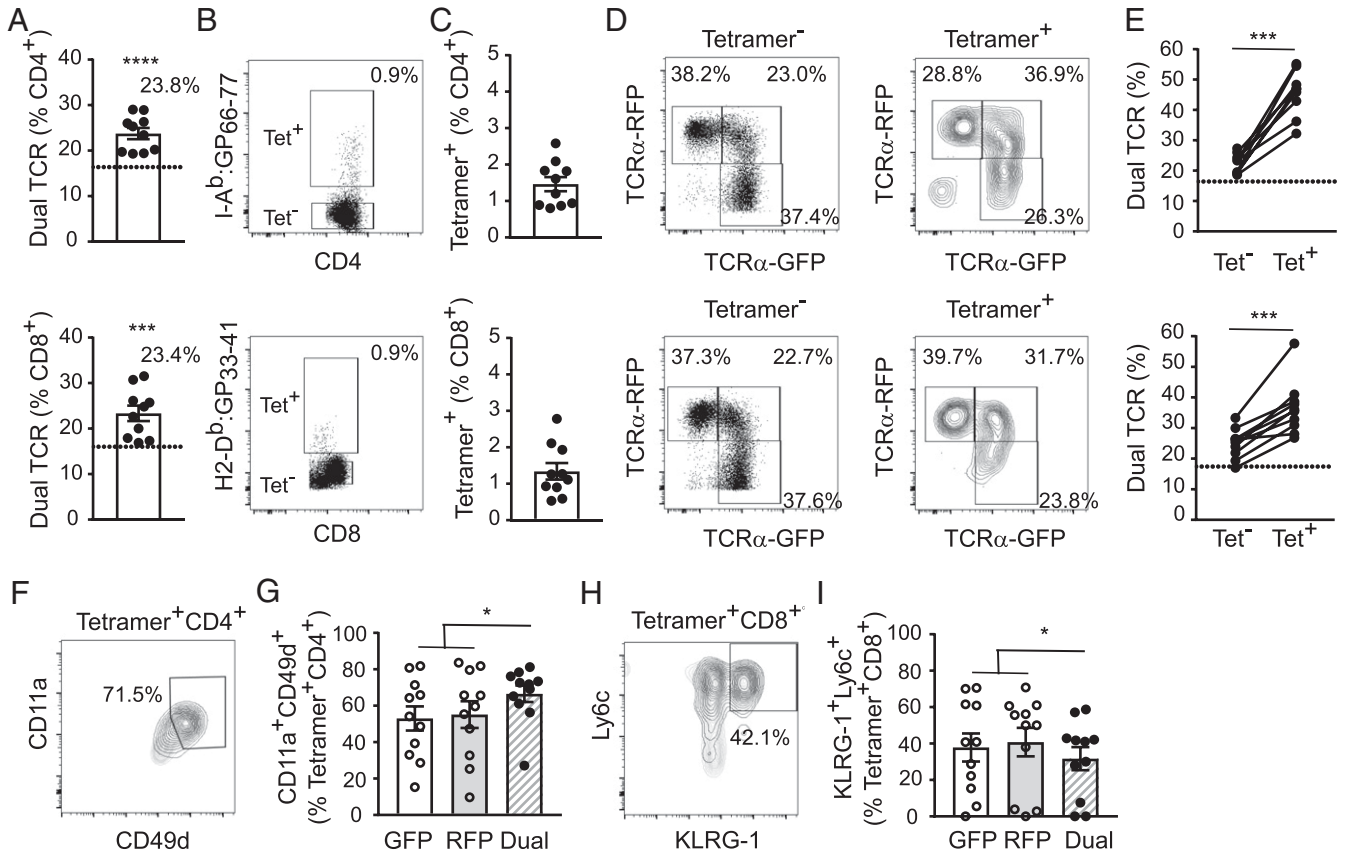


**Fig. 4.** Dual TCR cells are selectively increased in response to LCMV infection. All data represent 11 individual mice from three independent experiments. (*A*) B6.TCRA-GFP/RFP mice were infected i.v. with $2 \times 10^5$ plaque-forming units LCMV Armstrong and dual TCRα cells were measured by flow cytometry of splenocytes and lymph node cells 8 d after infection. Dots represent individual mice with mean ± SEM. Data compared to immunologically naive mice (dotted line) nonparametrically by Mann–Whitney *U* test. (*B*) LCMV-specific T cells were identified by flow cytometry for binding I-$A^b$:$GP_{66–77}$ and H2-$D^b$:$GP_{33–41}$ tetramers. Representative samples shown. (*C*) Quantification of LCMV-tetramer–binding cells in LCMV infected mice. Dots represent individual mice with mean ± SEM. (*D*) Flow cytometry to identify dual TCRα $CD4^+$ and $CD8^+$ T cells from tetramer (Tet)$^+$ and $Tet^-$ cells. Representative sample shown. (*E*) Comparison of dual TCRα T cells among $Tet^-$ and $Tet^+$ $CD4^+$ and $CD8^+$ T cells from LCMV-infected mice. Linked dots represent $Tet^-$ and $Tet^+$ cells from individual mice. Dotted line represents mean dual TCRα cell frequencies from naive mice. Comparison of $Tet^+$ and $Tet^-$ dual TCRα frequencies within individual samples performed nonparametrically using Wilcoxon matched-pairs rank-sign test. (*F*) Activated $CD4^+$ T cells present 8 d after LCMV infection were identified from $Tet^+$ cells by flow cytometry for expression of CD11a and CD49d. Gray lines are total $CD4^+$ cells and dark lines are gated on $Tet^+$ cells. Representative sample shown. (*G*) Quantification of $CD4^+Tet^+CD11a^+CD49d^+$ activated T cells. Dots represent individual mice with mean ± SEM. Data compared within individual samples nonparametrically using Wilcoxon matched-pairs rank-sign test. (*H*) Effector $CD8^+$ T cells present 8 d after LCMV infection were identified from $Tet^+$ cells by flow cytometry for expression of Ly6c and KLRG-1. Gray lines are total $CD8^+$ cells and dark lines are gated on $Tet^+$ cells. Representative sample shown. (*I*) Quantification of $CD8^+Tet^+KLRG\text{-}1^+Ly6c^+$ effector T cells. Dots represent individual mice with mean ± SEM. Data compared within individual samples nonparametrically using Wilcoxon matched-pairs rank-sign test. $^*P < 0.05$, $^{***}P < 0.005$, $^{****}P < 0.001$.

long-term fate of $CD4^+$ T cell function during protective immune response and may promote $CD4^+$ memory formation.

## Discussion

These data uncover unappreciated roles for dual TCRα expression in the function of the immune system. The physiologic impact of dual TCRα expression has been debated, as genetic elimination of dual TCRα coexpression (as in $TCRC\alpha^{+/-}$ mice) does not broadly change the composition of peripheral T cell numbers or subsets and does not completely eliminate reactivity against any antigen tested. This singularly reductionist view represents an unachievable standard, as the breadth of the TCR repertoire (46) and the flexibility with which TCRs interact with pMHC ligands (47) are likely to preclude absolute "present or absent" effects of changes to the TCR repertoire. Our approach enabled unambiguous identification of single and dual TCRα cells from the intact T cell repertoire, defining the dual TCRα cell subset as ∼16% of peripheral T cells in immunologically naive adult mice (Fig. 1). This is significantly higher than traditional estimates of 1 to 10% (2, 10) and in line with our recent description of ∼18% of T cells from healthy adult humans having two in-frame *TRAV-J* gene rearrangements identified by single-cell RNA sequencing (22).

Generation of T cells coexpressing two TCRα proteins results from the simultaneous rearrangement of both TCRα loci in DP thymocytes. Allelic inclusion of TCRα has been demonstrated to facilitate positive selection (8, 19), though it is undefined whether this depends on generation of two TCRα proteins or if it reflects an increased efficiency of having twice the opportunity to generate a TCRα protein capable of pairing with TCRβ and responding to the limited repertoire of selecting self-pMHC ligands in the thymic cortex. Our data demonstrating that thymocytes expressing two TCRα proteins are significantly increased among $TCR^{high}$ postselection DP thymocytes (Fig. 2) suggest that the benefit of TCRα allelic inclusion is associated with coexpression of two TCRα proteins, rather than an increased efficiency of generating a single productive TCRα. Transgenic TCR systems have demonstrated that dual TCR coexpression can have either

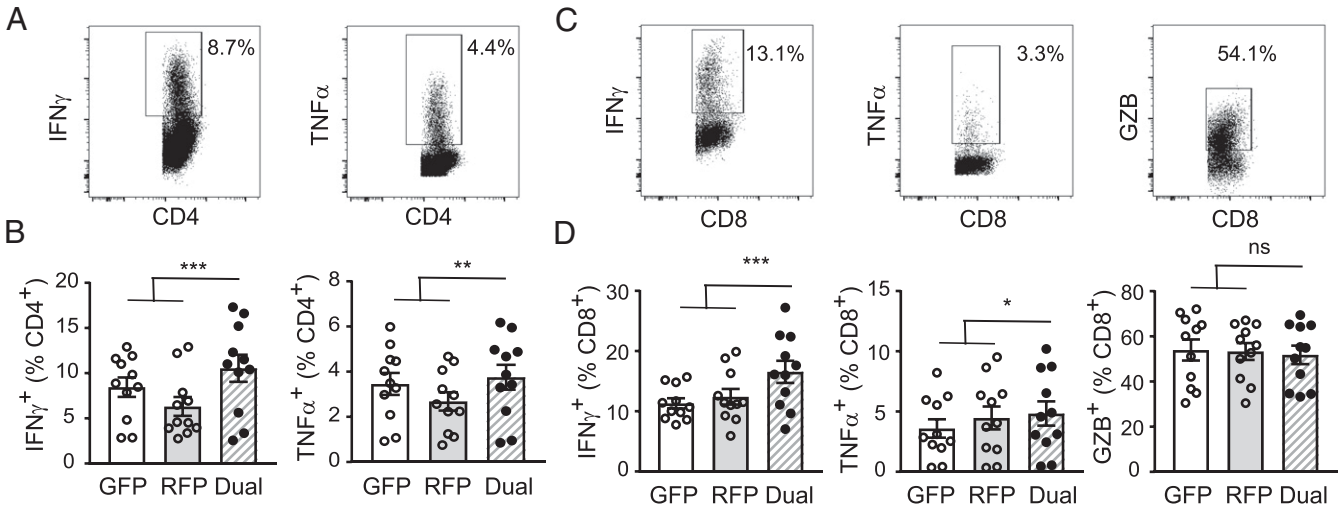


**Fig. 5.** Dual TCR cells have increased functional response to LCMV. All data represent 11 individual mice from three independent experiments. (*A*) Cytokine production of $CD4^+$ T cells from LCMV-infected mice was assessed 8 d postinfection by intracellular flow cytometry after ex vivo stimulation of splenocytes with LCMV $GP_{66–77}$ peptide. Representative sample shown. (*B*) Quantification of IFNγ- and TNFα-producing cells for TCRA-$GFP^+$, TCRA-$RFP^+$, and TCRA-$GFP^+RFP^+$ cells. Dots represent individual mice with mean ± SEM. Data compared within individual samples nonparametrically using Wilcoxon matched-pairs rank-sign test. (*C*) Cytokine production of $CD8^+$ T cells from LCMV-infected mice was assessed by intracellular flow cytometry after ex vivo stimulation of splenocytes with LCMV $GP_{33–41}$ peptide. Representative sample shown. (*D*) Quantification of IFNγ-, TNFα-, and granzyme B (GZB)-producing cells for TCRA-$GFP^+$, TCRA-$RFP^+$, and TCRA-$GFP^+RFP^+$ cells. Dots represent individual mice with mean ± SEM. Data compared within individual samples nonparametrically using Wilcoxon matched-pairs rank-sign test. $*P < 0.05$, $**P < 0.01$, $***P < 0.005$; ns = not statistically significant.

potentiating or inhibitory effects on TCR signaling in response to agonist ligand (48–50). Our current data do not indicate that dual TCRα expression affects the strength of the signal with positively selecting ligands, as expression of CD5 is unaffected by dual TCRα expression on mature thymocytes (*SI Appendix*, Fig. S3). However, CD5 is only a surrogate marker and future studies examining TCR signaling pathways and more discriminatory measures of TCR signal strength such as Nur77 (51) will be important

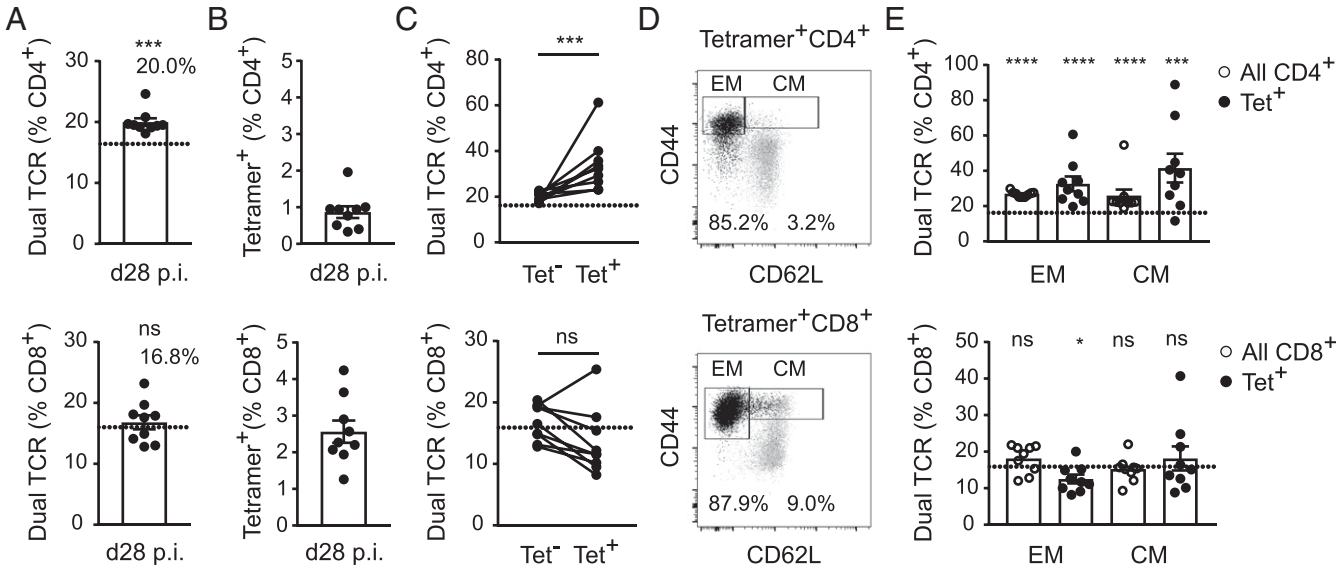


**Fig. 6.** Dual TCR expression affects persistence of LCMV-specific cells after infection. All data represent nine individual mice from three independent experiments. (*A*) Dual TCR cell response assessed by flow cytometry of splenocytes and lymph node cells 28 d after infection of B6.TCRA-GFP/RFP mice with $2 \times 10^5$ plaque-forming units LCMV Armstrong. Dots represent individual mice with mean ± SEM. Data compared to immunologically naive mice (dotted line) nonparametrically by Mann–Whitney *U* test. (*B*) Quantification of LCMV I-$A^b$:$GP_{66–77}$ and H2-$D^b$:$GP_{33–41}$ tetramer (Tet)-binding cells. Dots represent individual mice with mean ± SEM. (*C*) Comparison of dual TCRα T cells among $Tet^-$ and $Tet^+$ $CD4^+$ and $CD8^+$ T cells. Linked dots represent $Tet^-$ and $Tet^+$ cells from individual mice. Dotted line represents mean dual TCRα cell frequencies from naive mice. Comparison of $Tet^+$ and $Tet^-$ dual TCRα frequencies within individual samples performed nonparametrically using Wilcoxon matched-pairs rank-sign test. (*D*) LCMV-specific EM and CM cells identified from $CD4^+$ and $CD8^+Tet^+$ cells by flow cytometry. Gray lines are total $CD4^+$ or $CD8^+$ cells and dark lines are gated on $Tet^+$ cells. Representative sample shown. (*E*) Quantification of dual TCR cells in EM and CM subsets for total (open circles) or $Tet^+$ (closed circles) T cells. Dots represent individual mice with mean ± SEM. Groups compared to dual TCR cell frequencies from naive mice (dotted line) nonparametrically using Mann–Whitney *U* test. $*P < 0.05$, $***P < 0.005$, $****P < 0.001$; ns = not statistically significant.

to more thoroughly evaluate this. In similar form, dual TCRα expression does not seem to promote agonist selection (Fig. 2 and *SI Appendix*, Fig. S3). Data from a *TRAC*$^{+/-}$ model have demonstrated that TCRα coexpression impairs agonist selection of Tregs (19). It was hypothesized that this occurred via alteration of TCR signal strength in response to positively selecting pMHC. Future studies using our model to dissect how TCRα coexpression affects TCR signaling during thymocyte development and whether this imprints future functional ability on dual TCRα cells will be important for understanding this process.

The robust ability of our model to identify dual TCRα cells enabled discovery of their function during a physiologic immune response. LCMV Armstrong infection experiments revealed that dual TCRα cells were unexpectedly prominent contributors to the antiviral immune response, as measured by recognizing I-A$^b$:GP$_{66–77}$ and H2-D$^b$:GP$_{33–41}$ tetramers, as well as by ex vivo stimulation of cells with LCMV GP$_{66–77}$ and GP$_{33–41}$ antigens (Figs. 4 and 5). Expansion of dual TCRα cells during acute infection also extended outside of cells reactive to these antigens (Fig. 4). It remains to be determined whether this represents selective dual TCRα responses against other LCMV antigens or if dual TCRα cells are expanding via off-target or bystander activation. This difference could have important consequences related to epitope spreading and heterologous immunity. Our work demonstrating the alloreactive potential of dual TCRα cells would suggest that this risk could extend to heterologous immune responses against alloantigens, which could present significant risk for transplant rejection or graft-versus-host disease.

The mechanism through which dual TCRα cells are selectively increased in number and function during an immune response is unclear. An intuitive notion that coexpression of two TCR clonotypes could broaden the antigenic reactivity of a given T cell would suggest that dual TCRα cells are expanded in response to infection simply because they have a second opportunity to recognize a viral antigen. However, we have previously demonstrated that dual receptor cells contain a unique subset of TCRs (8). These are presumably TCR clonotypes that would otherwise be removed during thymic selection but instead emerge as coexpressed with TCRs capable of independently mediating positive selection or downregulating or "masking" the cross-reactive or autoreactive TCR from negative selection (9, 11, 14, 15, 17). This implies that dual TCRα cells potentially harbor highly cross-reactive or self-reactive TCRs (52, 53). The broad expansion of dual TCRα cells not specific for LCMV GP$_{66–77}$ and GP$_{33–41}$ antigens (Fig. 4) may be partly a result of this type of cross-reactivity, in addition to reactivity against other LCMV epitopes. Further studies to interrogate the biochemistry of ligand recognition by dual TCR cells participating in immune responses are necessary.

The data here present evidence that coexpression of dual TCRs can have qualitatively different effects for CD4$^+$ and CD8$^+$ T cells during an immune response. Both CD4$^+$ and CD8$^+$ dual TCRα cells expanded robustly during the acute immune response (Fig. 4), but CD4$^+$ dual TCRα cells remained significantly increased among LCMV-specific cells at 28 d after infection, while LCMV-specific CD8$^+$ cells returned to baseline frequencies (Fig. 6). Both LCMV-specific CD8$^+$ and CD4$^+$ T cells were predominantly EM cells, with a significant contribution of CM cells, though only in CD4$^+$ T cells were the postinfection EM and CM compartments enriched for dual TCRα cells (Fig. 6). This difference may reflect the different kinetics of expansion and contraction of virus-specific cells, with a delayed contraction of CD4$^+$ LCMV-specific cells compared to CD8$^+$ cells (41). However, the quality of TCR–ligand interaction affects T cell effector function, determination of the responding T cell repertoire, and potential for memory formation (54, 55). In LCMV infection, CD4$^+$ cell function has been positively correlated with affinity for viral antigens (56), and the results presented here could reflect an increased function of dual TCRα cells after infection driven by higher affinity for viral antigens. Again, biochemical studies of ligand recognition by dual TCRα cells are necessary to evaluate this possibility.

An alternate hypothesis for the effect of dual TCRα expression on T cell function during acute infection and selective promotion of memory cells after the resolution of infection is that this may result from an increased potential for reactivity against self-pMHC ligands, rather than differential affinity for viral antigens. Results from other models indicate that reactivity of TCR for self-pMHC ligands, including as evidenced by increased expression of CD5, correlates with the formation and persistence of protective CD4$^+$ T cell responses and memory formation (39, 57–59). Here (Fig. 3), as well as in prior studies (35), we have identified that dual TCRα cells express higher levels of CD5 than single TCRα cells and that this difference is more pronounced in CD4$^+$ dual TCRα cells. We have previously confirmed the functional impact of this in acute lymphopenia-induced proliferation, a recognized effect of affinity for self-pMHC (35). This difference in peripheral T cells is in contrast to a lack of observable difference in CD5 expression between single and dual TCRα CD4SP and CD8SP (*SI Appendix*, Fig. S3). However, CD5 expression can change in response to self-pMHC–induced tonic signaling in the periphery (39). We propose this difference may be related to a more narrow window of permissive reactivity against self-pMHC in the thymus compared to the periphery. It may also result from a wider range of self-antigens present in peripheral tissues as compared to the thymus. Mechanisms potentially underlying how dual TCR coexpression affects reactivity against self-ligands, including not only the potential for autoreactivty but also coagonism and TCR signal attenuation by CD5, are essential questions for continued study.

## Materials and Methods

**Mice.** C57BL/6 mice were originally purchased from Charles River Laboratories. Mice with fluorescent reporters linked to the TCRCα protein were generated by CRISPR-Cas9–mediated recombination (*SI Appendix, Supplemental Methods*). B6.TCRA-GFP/RFP mice were generated by interbreeding B6.TCRA-GFP and B6.TCRA-RFP mice. Both male and female mice were used in this study. Age- and sex-matched mice of 6 to 8 wk of age were used for all studies. All experimental mice were bred and housed in specific-pathogen-free conditions in a 12-h light/dark cycle with ad libitum access to chow and water at the University of California San Diego (UCSD). All breeding and experiments were performed according to UCSD Institutional Animal Care and Use Committee–approved protocols and under the supervision of the UCSD Animal Care Program.

**Flow Cytometry.** Cells were incubated with Zombie yellow (Biolegend) viability dye prior to labeling with antibodies as indicated. Samples were run in batches containing control and experimental samples with color and fluorescence-minus-one (FMO) controls. Where applicable, cells from single-transgenic B6.TCRA-GFP and B6.TCRA-RFP mice were used as FMO controls for gating single and dual TCR cells from B6.TCRA-GFP/RFP mice. Flow cytometry analyses were performed using FACSCanto or LSR II instruments (BD Biosciences) with FACSDiva software. Data were analyzed using FlowJo v10 software.

**Confocal Microscopy.** T cells were isolated by negative paramagnetic bead selection and directly plated in Nunc Lab-Tek chambered coverglass. Confocal imaging was performed using Olympus FV1000 confocal microscope (Olympus America) at 600× magnification. GFP (excitation: 488 nm, filter: 500 nm to 530 nm) and RFP (excitation: 543 nm, filter: 555 nm to 655 nm) channels were scanned in sequential-frame manner to exclude overlapping. Ten independent fields containing 300 to 1,000 cells per field were taken for each mouse. Images were processed and analyzed using ImageJ Fiji software (60).

**In Vitro T Cell Proliferation.** Peripheral T cells were isolated from spleens using negative paramagnetic bead selection and labeled with Tag-it Violet tracking dye (Biolegend). T cells were cultured in vitro in RPMI 1640 supplemented with 10% fetal bovine serum, 2 mM Glutamax, and 0.5 μg/mL gentamicin

(Thermo Scientific) in 96-well flat-bottomed plates. Cells were stimulated with graded doses of plate-bound anti-CD3 (2C.11)/anti-CD28 (37.51) mAbs and SEB as indicated and cultured for 5 d at 37 °C 6% $CO_2$. Proliferation was measured by flow cytometry and proliferation index was calculated as the total number of cell divisions divided by calculated number of divided cells (61).

**LCMV Infection.** LCMV Armstrong strain was propagated on BHK cells and quantified by plaque assay performed on Vero cells. Vero cell monolayers were infected with 500 mL serially diluted viral stock and incubated for 60 min at 37 °C, 5% $CO_2$ with gentle shaking. Agarose overlay was applied to infected cells and incubated at 37 °C, 5% $CO_2$ for 6 d, after which cells were fixed with formaldehyde and stained with crystal violet for 5 min at room temperature for plaque enumeration. Mice were infected by intravenous (i.v.) injection of $2 \times 10^5$ plaque forming units of murine LCMV Armstrong strain. Mice were killed 8 or 28 d after infection, and spleen and lymph nodes were collected for analysis by flow cytometry. LCMV-specific T cells were identified by flow cytometry for pMHC-tetramer labeling for $GP_{33–41}$ (KAVYNFATM):H2-$D^b$ and $GP_{66–77}$ (DIYKGVYQFKSV):I-$A^b$ (NIH Tetramer Core). Tetramer labeling was performed by 30′ incubation of cells (labeled with viability dye) with 1:100 dilution of tetramer at room temperature. Cells were subsequently labeled with mAb, including antibodies against B220, F4/80, CD11c, and CD11b to exclude nonspecific tetramer binding.

**Statistical Analyses.** Data were analyzed using Prism 6 software. Data from individual mice were analyzed nonparametrically using Mann–Whitney *U* test. Analysis of intersample groups was performed nonparametrically using Wilcoxon matched-pairs rank-sign test. Proliferation indices were compared between groups across graded stimulation using two-way ANOVA with Tukey's multiple comparison test. Mean fluorescence intensity (MFI) values from intersample groups were compared using paired Student's *t* test for mean values. Two-tailed *P* values $\leq 0.05$ were considered statistically significant for all analyses.

**Data Availability.** All study data are included in the paper and *SI Appendix*.

**ACKNOWLEDGMENTS.** We thank Wei Feng (UCSD) and Ella Kothari and Jun Zhao (UCSD Transgenic Mouse Shared Resource) for assistance in CRISPR-Cas9 blastocyst microinjection, Cody Fine and Jesus Olivera (UCSD Human Embryonic Stem Cell Core Facility) for assistance in flow cytometry cell sorting, Jack Bui (UCSD) for use of flow cytometry equipment, and Paul M. Allen (Washington University) and Wan-Lin Lo (UCSF) for helpful discussion and comments. This research was supported by NIH R56 AI137150 (G.P.M.), R01 AI151293 (G.P.M.), R01 AI081923 (E.I.Z.), and an American Society of Hematology Bridge grant (G.P.M.). The UCSD Human Embryonic Stem Cell Core Facility is supported by California Institute for Regenerative Medicine Major Facilities Grant FA1-00607.

1. G. P. Morris, P. M. Allen, How the TCR balances sensitivity and specificity for the recognition of self and pathogens. *Nat. Immunol.* **13**, 121–128 (2012).
2. E. Padovan *et al*., Expression of two T cell receptor α chains: dual receptor T cells. *Science* **262**, 422–424 (1993).
3. E. Padovan *et al*., Normal T lymphocytes can express two different T cell receptor β chains: Implications for the mechanism of allelic exclusion. *J. Exp. Med.* **181**, 1587–1591 (1995).
4. S. M. Alam, I. N. Crispe, N. R. Gascoigne, Allelic exclusion of mouse T cell receptor α chains occurs at the time of thymocyte TCR up-regulation. *Immunity* **3**, 449–458 (1995).
5. J. L. Casanova, P. Romero, C. Widmann, P. Kourilsky, J. L. Maryanski, T cell receptor genes in a series of class I major histocompatibility complex-restricted cytotoxic T lymphocyte clones specific for a Plasmodium berghei nonapeptide: Implications for T cell allelic exclusion and antigen-specific repertoire. *J. Exp. Med.* **174**, 1371–1383 (1991).
6. P. Borgulya, H. Kishi, Y. Uematsu, H. von Boehmer, Exclusion and inclusion of α and β T cell receptor alleles. *Cell* **69**, 529–537 (1992).
7. H. T. Petrie *et al*., Multiple rearrangements in T cell receptor alpha chain genes maximize the production of useful thymocytes. *J. Exp. Med.* **178**, 615–622 (1993).
8. P. P. Ni, B. Solomon, C. S. Hsieh, P. M. Allen, G. P. Morris, The ability to rearrange dual TCRs enhances positive selection, leading to increased Allo- and Autoreactive T cell repertoires. *J. Immunol.* **193**, 1778–1786 (2014).
9. F. Hardardottir, J. L. Baron, C. A. Janeway Jr, T cells with two functional antigen-specific receptors. *Proc. Natl. Acad. Sci. U.S.A.* **92**, 354–358 (1995).
10. J. I. Elliott, D. M. Altmann, Dual T cell receptor α chain T cells in autoimmunity. *J. Exp. Med.* **182**, 953–959 (1995).
11. T. Zal, S. Weiss, A. Mellor, B. Stockinger, Expression of a second receptor rescues self-specific T cells from thymic deletion and allows activation of autoreactive effector function. *Proc. Natl. Acad. Sci. U.S.A.* **93**, 9102–9107 (1996).
12. A. Sarukhan, C. Garcia, A. Lanoue, H. von Boehmer, Allelic inclusion of T cell receptor α genes poses an autoimmune hazard due to low-level expression of autospecific receptors. *Immunity* **8**, 563–570 (1998).
13. X. He *et al*., Dual receptor T cells extend the immune repertoire for foreign antigens. *Nat. Immunol.* **3**, 127–134 (2002).
14. G. P. Morris, P. M. Allen, Cutting edge: Highly alloreactive dual TCR T cells play a dominant role in graft-versus-host disease. *J. Immunol.* **182**, 6639–6643 (2009).
15. Q. Ji, A. Perchellet, J. M. Goverman, Viral infection triggers central nervous system autoimmunity via activation of $CD8^+$ T cells expressing dual TCRs. *Nat. Immunol.* **11**, 628–634 (2010).
16. E. Kekäläinen, A. Hänninen, M. Maksimow, T. P. Arstila, T cells expressing two different T cell receptors form a heterogeneous population containing autoreactive clones. *Mol. Immunol.* **48**, 211–218 (2010).
17. J. L. Auger, S. Haasken, E. M. Steinert, B. A. Binstadt, Incomplete TCR-β allelic exclusion accelerates spontaneous autoimmune arthritis in K/BxN TCR transgenic mice. *Eur. J. Immunol.* **42**, 2354–2362 (2012).
18. G. P. Morris, G. L. Uy, D. Donermeyer, J. F. Dipersio, P. M. Allen, Dual receptor T cells mediate pathologic alloreactivity in patients with acute graft-versus-host disease. *Sci. Transl. Med.* **5**, 188ra74 (2013).
19. N. J. Schuldt *et al*., Cutting edge: Dual TCRα expression poses an autoimmune hazard by limiting regulatory T cell generation. *J. Immunol.* **199**, 33–38 (2017).
20. D. A. Bolotin *et al*., MiTCR: Software for T-cell receptor sequencing data analysis. *Nat. Methods* **10**, 813–814 (2013).
21. A. Han, J. Glanville, L. Hansmann, M. M. Davis, Linking T-cell receptor sequence to functional phenotype at the single-cell level. *Nat. Biotechnol.* **32**, 684–692 (2014).
22. A. Balakrishnan, N. Gloude, R. Sasik, E. D. Ball, G. P. Morris, Proinflammatory dual receptor T cells in chronic graft-versus-host disease. *Biol. Blood Marrow Transplant.* **23**, 1852–1860 (2017).
23. S. M. Alam, N. R. Gascoigne, Posttranslational regulation of TCR Valpha allelic exclusion during T cell differentiation. *J. Immunol.* **160**, 3883–3890 (1998).
24. H. Yang, H. Wang, R. Jaenisch, Generating genetically modified mice using CRISPR/Cas-mediated genome engineering. *Nat. Protoc.* **9**, 1956–1968 (2014).
25. B. F. Koop *et al*., Organization, structure, and function of 95 kb of DNA spanning the murine T-cell receptor C α/C δ region. *Genomics* **13**, 1209–1230 (1992).
26. R. S. Friedman, P. Beemiller, C. M. Sorensen, J. Jacobelli, M. F. Krummel, Real-time analysis of T cell receptors in naive cells *in vitro* and *in vivo* reveals flexibility in synapse and signaling dynamics. *J. Exp. Med.* **207**, 2733–2749 (2010).
27. A. Alcover, B. Alarcon, V. Di Bartolo, Cell biology of T cell receptor expression and regulation. *Ann. Rev. Immunol.* **36**, 103–125 (2018).
28. A. Monjas, A. Alcover, B. Alarcón, Engaged and bystander T cell receptors are down-modulated by different endocytotic pathways. *J. Biol. Chem.* **279**, 55376–55384 (2004).
29. E. Fernandez-Arenas, *et al*., β-Arrestin-1 mediates the TCR-triggered re-routing of distal receptors to the immunological synapse by a PKC-mediated mechanism. *EMBO J.* **33**, 559–577 (2014).
30. J. F. Huang *et al*., TCR-Mediated internalization of peptide-MHC complexes acquired by T cells. *Science* **286**, 952–954 (1999).
31. G. L. Stritesky, S. C. Jameson, K. A. Hogquist, Selection of self-reactive T cells in the thymus. *Annu. Rev. Immunol.* **30**, 95–114 (2012).
32. A. Tarakhovsky *et al*., A role for CD5 in TCR-mediated signal transduction and thymocyte selection. *Science* **269**, 535–537 (1995).
33. H. S. Azzam *et al*., CD5 expression is developmentally regulated by T cell receptor (TCR) signals and TCR avidity. *J. Exp. Med.* **188**, 2301–2311 (1998).
34. C. Sinclair, M. Saini, I. Schim van der Loeff, S. Sakaguchi, B. Seddon, The long-term survival potential of mature T lymphocytes is programmed during development in the thymus. *Sci. Signal.* **4**, ra77 (2011).
35. A. Balakrishnan, B. Jama, G. P. Morris, Endogenous co-expression of two T cell receptors promotes lymphopenia-induced proliferation via increased affinity for self-antigen. *J. Leukoc. Biol.* **104**, 1097–1104 (2018).
36. J. A. Punt, J. L. Roberts, K. P. Kearse, A. Singer, Stoichiometry of the T cell antigen receptor (TCR) complex: Each TCR/CD3 complex contains one TCR α, one TCR β, and two CD3 ε chains. *J. Exp. Med.* **180**, 587–593 (1994).
37. B. Ernst, D. S. Lee, J. M. Chang, J. Sprent, C. D. Surh, The peptide ligands mediating positive selection in the thymus control T cell survival and homeostatic proliferation in the periphery. *Immunity* **11**, 173–181 (1999).
38. A. W. Goldrath, M. J. Bevan, Low-affinity ligands for the TCR drive proliferation of mature $CD8^+$ T cells in lymphopenic hosts. *Immunity* **11**, 183–190 (1999).
39. S. P. Persaud, C. R. Parker, W. L. Lo, K. S. Weber, P. M. Allen, Intrinsic $CD4^+$ T cell sensitivity and response to a pathogen are set and sustained by avidity for thymic and peripheral complexes of self peptide and MHC. *Nat. Immunol.* **15**, 266–274 (2014).
40. L. A. Kalekar *et al*., CD4(+) T cell anergy prevents autoimmunity and generates regulatory T cell precursors. *Nat. Immunol.* **17**, 304–314 (2016).
41. D. Homann, L. Teyton, M. B. Oldstone, Differential regulation of antiviral T-cell immunity results in stable $CD8^+$ but declining $CD4^+$ T-cell memory. *Nat. Med.* **7**, 913–919 (2001).
42. D. S. McDermott, S. M. Varga, Quantifying antigen-specific CD4 T cells during a viral infection: CD4 T cell responses are larger than we think. *J. Immunol.* **187**, 5568–5576 (2011).
43. S. M. Kaech *et al*., Selective expression of the interleukin 7 receptor identifies effector CD8 T cells that give rise to long-lived memory cells. *Nat. Immunol.* **4**, 1191–1198 (2003).
44. J. J. Sabatino, Jr, J. Huang, C. Zhu, B. D. Evavold, High prevalence of low affinity peptide-MHC II tetramer-negative effectors during polyclonal $CD4^+$ T cell responses. *J. Exp. Med.* **208**, 81–90 (2011).

45. C. Rius *et al*., Peptide-MHC class I tetramers can fail to detect relevant functional T cell clonotypes and underestimate antigen-reactive T cell populations. *J. Immunol.* **200**, 2263–2279 (2018).
46. H. S. Robins *et al*., Comprehensive assessment of T-cell receptor β-chain diversity in alphabeta T cells. *Blood* **114**, 4099–4107 (2009).
47. L. A. Colf *et al*., How a single T cell receptor recognizes both self and foreign MHC. *Cell* **129**, 135–146 (2007).
48. J. M. Robertson, B. D. Evavold, Cutting edge: Dueling TCRs: Peptide antagonism of $CD4^+$ T cells with dual antigen specificities. *J. Immunol.* **163**, 1750–1754 (1999).
49. B. N. Dittel, I. Stefanova, R. N. Germain, C. A. Janeway Jr, Cross-antagonism of a T cell clone expressing two distinct T cell receptors. *Immunity* **11**, 289–298 (1999).
50. R. M. Teague *et al*., Peripheral $CD8^+$ T cell tolerance to self-proteins is regulated proximally at the T cell receptor. *Immunity* **28**, 662–674 (2008).
51. A. E. Moran *et al*., T cell receptor signal strength in Treg and iNKT cell development demonstrated by a novel fluorescent reporter mouse. *J. Exp. Med.* **208**, 1279–1289 (2011).
52. E. S. Huseby, F. Crawford, J. White, J. Kappler, P. Marrack, Negative selection imparts peptide specificity to the mature T cell repertoire. *Proc. Natl. Acad. Sci. U.S.A.* **100**, 11565–11570 (2003).
53. B. D. McDonald, J. J. Bunker, S. A. Erickson, M. Oh-Hora, A. Bendelac, Crossreactive αβ T cell receptors are the predominant targets of thymocyte negative selection. *Immunity* **43**, 859–869 (2015).
54. E. Corse, R. A. Gottschalk, J. P. Allison, Strength of TCR-peptide/MHC interactions and *in vivo* T cell responses. *J. Immunol.* **186**, 5039–5045 (2011).
55. N. J. Tubo *et al*., Single naive $CD4^+$ T cells from a diverse repertoire produce different effector cell types during infection. *Cell* **153**, 785–796 (2013).
56. M. A. Williams, E. V. Ravkov, M. J. Bevan, Rapid culling of the $CD4^+$ T cell repertoire in the transition from effector to memory. *Immunity* **28**, 533–545 (2008).
57. I. Stefanová, J. R. Dorfman, R. N. Germain, Self-recognition promotes the foreign antigen sensitivity of naive T lymphocytes. *Nature* **420**, 429–434 (2002).
58. J. N. Mandl, J. P. Monteiro, N. Vrisekoop, R. N. Germain, T cell-positive selection uses self-ligand binding strength to optimize repertoire recognition of foreign antigens. *Immunity* **38**, 263–274 (2013).
59. R. B. Fulton *et al*., The TCR's sensitivity to self peptide-MHC dictates the ability of naive $CD8(^+)$ T cells to respond to foreign antigens. *Nat. Immunol.* **16**, 107–117 (2015).
60. J. Schindelin *et al*., Fiji: An open-source platform for biological-image analysis. *Nat. Methods* **9**, 676–682 (2012).
61. M. Roederer, Interpretation of cellular proliferation data: Avoid the panglossian. *Cytometry A* **79**, 95–101 (2011).